Sparseness of the trabecular pattern on dental radiographs: visual assessment compared with semi-automated measurements

Geraets, W.G.M.; Lindh, C.; Verheij, H.

DOI
10.1259/bjr/32962542

Publication date
2012

Document Version
Author accepted manuscript

Published in
British Journal of Radiology

Sparseness of the Trabecular Pattern on Dental Radiographs: Visual Assessment compared with Semi-Automated Measurements

Corresponding author:
Dr. Wil GM Geraets, MSc, PhD
Department of Oral and Maxillofacial Radiology
Academic Centre for Dentistry Amsterdam (ACTA)
Gustav Mahlerlaan 3004
1081 LA Amsterdam
The Netherlands
W.Geraets@acta.nl
tel: +20 - 59 80831

Prof. Christina Lindh
Department of Oral Radiology Faculty of Odontology
Malmö University
SE - 205 06 Malmö
Sweden
Christina.Lindh@mah.se

Dr. Hans Verheij, MSc, PhD
Department of Oral and Maxillofacial Radiology
Academic Centre for Dentistry Amsterdam (ACTA)
Gustav Mahlerlaan 3004
1081 LA Amsterdam
The Netherlands
H.Verheij@acta.nl

Reported work was carried out in Amsterdam and Malmö

Short title: **Sparseness of the Trabecular Pattern on Dental Radiographs**

Acknowledgements

This work was supported by a research and technological development project grant from the European Commission Fifth Framework Programme 'Quality of Life and Management of Living Resources' (QLK6-2002-02243; 'Osteodent'). Thanks to Prof. Paul Van der Stelt (Academic Centre for Dentistry Amsterdam, The Netherlands), Prof. Keith Horner, Dr.Hugh Devlin, Prof. Judith Adams and Dr. Elisabeth Marjanovic (University of Manchester, United Kingdom), Prof. Reinhilde Jacobs (KU Leuven, Belgium), Prof. Kety Nicopoulou-Karayianni (University of Athens, Greece), for organizing the project, recruiting patients and making the radiographs.

Sparseness of the Trabecular Pattern on Dental Radiographs: Visual Assessment compared with Semi-Automated Measurements

Abstract

Objective: In diagnostic imaging the human perception is the most prominent yet least studied source of error. Better understanding of image perception will help to improve diagnostic performance. This study focusses on the perception of coarseness of trabecular patterns on dental radiographs. Comparison of human vision with machine vision should yield knowledge on human perception.

Material and Method: In a study on identifying osteoporotic patients dental radiographs were made from 505 postmenopausal women 45 to 70 years of age. Intraoral radiographs of the lower and upper jaws were made. Five observers graded the trabecular pattern in categories dense, sparse or mixed. The 5 gradings were combined into a single averaged observer score per jaw. The radiographs were scanned and a region of interest (ROI) was indicated on each. The ROI's were processed with image analysis software measuring 25 image features. Pearson correlation and multiple linear regression were used to compare the averaged observer score with the image features.

Results: Fourteen image features correlated significantly with the observer judgement for both jaws. The strongest correlation was found for the average gray value in the ROI. Other features describing that osteoporotic patients have less but bigger marrow spaces than controls correlated less with the sparseness of the trabecular pattern than a rather crude measure for structure such as the average gray value.

Conclusion: Human perception of the sparseness of trabecular patterns is based more on average gray value of the ROI than on geometric details within the ROI.

Keywords:

Dental radiographs,	trabecular pattern,	psychophysics,
sparseness,	observer grading,	image processing.

Introduction

Image perception is an important aspect of diagnostic imaging [1, 2]. According to the UNSCEAR 2000 report (Annex D) the average number of diagnostic radiological examinations in countries with level I healthcare is about 1,000 per year per 1,000 population. Therefore it can be estimated that each European has about one radiological examination per year.

The interpretation of radiographs is complicated by the variations in human anatomy and the spatial information that is lost while projecting the patient body on a 2D plane [3]. Visual clues are overlooked or misinterpreted [4-6]. The diagnostic process of radiologists can be improved by the use of computers [7-11]. Pattern-recognition techniques have been designed to draw the attention of the radiologist to regions in mammograms that need careful scrutiny and interpretation [12]. Fully automated methods can screen chest radiographs for features of tuberculosis [13]. Although the results compete with human performance, the automated methods do not outperform the radiologists. It is expected that some day computers may replace human observers in the analysis of the data, however, complete replacement of the human observer is yet a remote possibility [11]. For the foreseeable future, human interpretation will continue to be an inseparable element of medical imaging [14]. We need to understand the images and the technologies used to acquire and display them, but since patient treatment and care depend a lot on radiologists interpreting images, we also need to understand human perception and cognition. In the process of image acquisition, image processing and image display many parameters are involved and it is largely unknown how they should be optimized for human interpretation. Understanding the perceptual and cognitive processes involved in reading medical images will help to enhance the most useful properties of the images to improve diagnostic performance and reduce error rates [2, 3, 6, 14-17].

In dental radiography many radiographs show bone with radiographic trabecular pattern, an irregular meshwork of vague bright lines with fuzzy dark meshes (Figure 1). Visual assessment of the trabecular pattern in intraoral radiographs is a method to identify women at risk of having

osteoporosis. Dense trabeculation is a strong indicator of healthy bone whereas sparse trabeculation is a sign of osteoporosis [18-20].

At the Oral Radiology department of the Academic Centre for Dentistry Amsterdam methods were developed for semi-automatic analysis of the trabecular pattern of radiographs. Measurements on the trabecular pattern of intraoral radiographs were found to predict bone mineral density and osteoporosis [21, 22].

When both the visual assessment and the semi automatic analysis had been applied to the same set of radiographs there rose an opportunity to compare the two and to gain more insight in the human perception of the coarseness of the radiographic trabecular pattern.

Materials and Methods

In 2003 the European Union granted a research project, named OSTEODENT, to five European Universities at Manchester, Amsterdam, Athens, Leuven, and Malmö.

Subjects and radiographs

In the project women from Manchester, Athens, Leuven and Malmö were recruited [20, 23]. Local ethical approval for the study was obtained in each recruiting centre and informed consent was obtained from all subjects. From each subject intraoral radiographs were made from the upper right and lower right premolar region using one of three Planmeca Prostyle Intra devices (60-63 kV; Planmeca Oy, Helsinki, Finland) or with a Siemens Heliodent MD (60 kV; Sirona, Bensheim, Germany). The radiographic trabecular pattern was graded by 3 experienced radiologists and 2 general practitioners [20].

They were given 3 reference images from the upper and the lower jaw and they were asked to classify the trabecular pattern between the roots of the premolars as dense, alternating dense and sparse, or sparse. Additional instructions to observers described dense trabeculation as

having many trabeculae connected to each other and small or few marrow spaces. Sparse trabeculation was described as having less trabeculae, larger marrow spaces, and darker. Any trabecular pattern that was ambiguous had to be assigned to the intermediate category. Lamina dura, mandibular cortex and maxillary sinus as well as diseased areas were excluded from the assessment.

Subjects that had not been graded by all the observers were excluded from the study [20]. Complete sets of data including BMD of hip and spine, two intraoral radiographs and 5 observer gradings were obtained from 505 subjects of which 21% was diagnosed as osteoporotic.

Image processing

The intraoral radiographs were scanned with a flatbed scanner (Agfa Duoscan T1200, Agfa Gevaert, Mortsel, Belgium; fixed sensitivity settings) at a resolution of 118 pixels cm^{-1} (300 dpi). Most radiographs displayed three interdental regions of which the widest was used by an observer to select a region of interest (ROI) containing trabecular pattern only (Figure 1). The ROI was subjected to automated image analysis procedures measuring various image features that have proven their relevance for bone structure and osteoporosis extensively [21-27]. First the mean (MEAN) and standard deviation (SD) of the gray values were determined on the raw unfiltered ROI (Figure 1).

Isolated pixels with deviating gray values were adjusted with a 3x3 median filter. Large scale variations in gray value caused by varying thickness of cortex and soft tissues were removed with an unsharp self-masking filter. Then the ROI was segmented using the mode of the histogram as threshold value. This resulted in a version of the ROI consisting of black and white segments (Figure 2). The segments were used to measure the fractal dimension according to the caliper method (FRACT), the number of black segments (N_{black}), the number, area and the perimeter of

the white segments (N_{white}, BV/TV, BS/TV) and an index of orientation in horizontal direction (0°) up to 165° in steps of 15° (LFD 0, LFD 15, ... LFD165).

Next the white segments were eroded to a wire frame that was used to measure length of the frame, number of terminal points and number of furcations (TSL_{white}, $N.Tm_{white}$, $N.Nd_{white}$). Similarly the black segments were eroded to a wire frame that was used to measure the length, number of terminal points and number of furcations (TSL_{black}, $N.Tm_{black}$, $N.Nd_{black}$). Various methods for filtering and measuring image features have been described before [21, 23-32]. Similar image features are current in studies on osteoporosis and bone structure [33-39].

Statistics

To reduce the variations between the individual gradings and to simplify the analysis the gradings of the five observers were combined by equating the gradings dense, alternating, and sparse with numbers 1, 2, and 3. For each subject and each jaw the five numbers were combined into a single averaged observer score, resulting in 1010 averaged observer scores pertaining to 505 subjects.

For the interobserver agreement values of the kappa index ranged from 0.32 (fair) to 0.55 (moderate) [20]. Since kappa is the agreement it can be seen that the disagreement, or noise, in the individual observer is 0.45 to 0.68. To estimate the noise in the averaged observer score the factor $1/\sqrt{(5)}$ is used leading to a noise level of 0.20 to 0.30. Obviously 30% of the variation in the averaged observer judgement must be considered noise and 70% of the variation in the averaged observer score is the maximum that can be accounted for by any set of features.

With respect to the image features it can be said that the semi-automatic measurements were very reproducible since most of the associated values of Cronbach's alpha exceeded 0.8 and even 0.9 [27].

To test the relation between the averaged observer score and the image features the Pearson correlation was calculated. In addition stepwise multiple linear regression was applied to calculate the multiple correlation between the averaged observer score and the image features. Single and multiple correlations were computed with the SPSS package (version 18, SPSS inc., Chicago, USA). To define significance $\alpha=0.05$ was used. Additional computations of confidence intervals were done in accordance with Hayes [40].

Results

Table 1 summarizes the correlations of the image features on the lower and upper jaws with the averaged observer score. Of the 25 features that were investigated 14 correlated significantly for both jaws and 6 correlated significantly for only one jaw. The difference between the correlation coefficients for upper jaw and the lower jaw was less than the critical value 0.124 for all features except BS/TV. Allowing 1 in 20 features to differ this implies that the corrrelations for upper and lower jaws correspond.

The highest correspondence is found for the average grayvalue (MEAN) in the lower jaw (-0.39), as well as in the upper jaw (-0.37). This implies that MEAN accounts for 15% of the variance in the averaged observer score in the lower jaw and 14% in the upper jaw.

Using stepwise multiple linear regression the percentage variation accounted for increased to 19% (R=0.43) for the upper jaw and 27% (R=0.52) for the lower jaw. The analysis started with predictor MEAN and then one by one predictors were added until the prediction improved insignificantly. Table 2 shows the predictors and the order in which they entered the regression eqation. For the lower jaw 6 predictors were entered and for the upper jaw 4. The three most important features in lower and upper jaw corresponded; they were MEAN, BS/TV and LFD 75.

Discussion

The assessments of the trabecular pattern by the observers were similar for the upper and lower jaw [20]. In addition the semi-automatic measurements of upper and lower jaws correspond to a large extent [29]. This may explain the correspondence of upper and lower jaws in Table 1.

In a previous study several features discriminated significantly between osteoporotic patients and healthy controls of which the strongest was the number of terminal points ($N.Tm_{black}$) [29]. To a large extent this is confirmed by the correlations provided in Table 1. It can be seen that the trabecular patterns of osteoporotic patients have less geometrical details than the patterns of the controls. Obviously osteoporotic patients have less but bigger marrow spaces than controls. This is consistent with the finding that sparse trabeculation is a sign of osteoporosis.

The negative value of the correlation between MEAN and the observer score implies that low values of MEAN are associated with sparse trabecular patterns which is consistent with the loss of bone mineral and increased sparseness of the radiographic trabecular pattern of osteoporotic patients [20,41]. Considering that MEAN represents the average gray value of the pixels in the ROI one might say that MEAN is a crude measure for structure. Therefore it is striking that in this study MEAN has a stronger correlation with the observer grading than the other features such as $N.Nd_{black}$ and TSL_{white} that reflect relevant structural aspects of trabecular microarchitecture. MEAN even surpasses features N_{black} and BV/TBV which are closely related with the concept of sparse and dense trabeculation. Part of a possible explanation can be found in the instructions to the observers stating that sparse trabeculation associates with darker images. Our main conclusion is that the human perception of the sparseness of trabecular patterns is based more on average gray value of the ROI than on other structural aspects of the ROI.

References

1. Bankman IN. Improvement of visual perception. In: Handbook of medical imaging. Processing and analysis. Academic press 2000; 788.

2. Krupinski EA, Kundel HL. Update on long-term goals for medical image perception research. Acad Radiol 1998; 5: 629-633.

3. Krupinski EA. The future of image perception in radiology: synergy between humans and computers. Acad Radiol 2003; 10: 1-3.

4. Gale A, Krupinsky EA, Manning DJ. Medical image perception society conference XI.
Br J Radiol 2006; 79: S109-S110.

5. Van Dijck JAM, Verbeek LM, Hendriks JHCL, Holland R. The current detectability of breast cancer in a mammographic screening program. Cancer 1993; 72: 1933-1938.

6. Krupinski EA. Medical image perception issues for PACS deployment. Semin Roentgenol 2003; 38: 231-243.

7. Kundel HL, Nodine CF, Krupinski EA. Computer-displayed eye position as a visual aid to pulmonary nodule recognition. Invest Radiol 1990; 25: 890-896

8. Nakamura K, Yoshida H, Engelmann R, MacMahon H, Katsuragawa S, Ishida T, et al. Computerized analysis of the likelihood of malignancy in solitary pulmonary nodules with use of artificial neural networks. Radiology 2000; 214: 823-830.

9. Floyd CE, Lo JY, Yun AJ, Sullivan DC, Kornguth PJ. Prediction of breast cancer malignancy using an artificial neural network. Cancer 1994; 74: 2944-2948.

10. Baker JA, Kornguth PJ, LO JY, Floyd CE. Artificial neural network: improving the quality of breast biopsy recommendations. Radiology 1996; 198: 131-135.

11. Robinson PJA. Radiology's Achilles'heel: error and variation in the interpretation of the Röntgen image. Br J Radiol 1997; 70: 1085-1098.

12. Te Brake GM, Karssemaijer JHCL. Automated detection of breast cancer carcinomas not detected in a screening program. Radiology 1998; 207: 465-471.

13. Van Ginneken B, Katsuragawa S, Ter Haar Romeny BM, Doi K, Viergever MA. Automatic detection of abnormalities in chest radiographs using local texture analysis. IEEE Trans Med Imaging 2002; 21: 139-148

14. Samei E. Why medical image perception? J Am Coll Radiol 2006; 3: 400-401.

15. Hendee WR, Wells PNT. Visual perception as an opportunity for radiologic research. Invest Radiol 1989; 24: 575-576.

16. Manning DJ, Gale A, Krupinsky EA. Perception research in medical imaging. Br J Radiol 2005; 78: 683-685.

17. Madsen MT, Berbaum KS, Ellingson AN, Thompson BH, Mullan BF, Caldwell RT. A new software tool for removing, storing and adding abnormalities to medical images for perception research studies. Acad Radiol 2006; 13: 305-312.

18. Jonasson G, Bankvall G, Kiliaridis S. Estimation of skeletal bone mineral density by means of the trabecular pattern of the alveolar bone, its interdental thickness, and the bone mass of the mandible. Oral Surg Oral Med Oral Pathol Oral Radiol Endod 2001; 92: 346-352.

19. Lindh C, Petersson A, Rohlin M. Assessment of the trabecular pattern before endosseous implant treatment. Diagnostic outcome of periapical radiography in the mandible. Oral Surg Oral Med Oral Pathol Oral Radiol Endod 1996; 82: 335-343.

20. Lindh C, Horner K, Jonasson G, Olsson P, Rohlin M, Jacobs R, et al. The use of visual assessment of dental radiographs for identifying women at risk of having osteoporosis: the OSTEODENT project. Oral Surg Oral Med Oral Pathol Oral Radiol Endod 2008; 106: 285-293.

21. Geraets WGM, Verheij JGC, Van der Stelt PF, Horner K, Lindh C, Nicopolou-Karayianni K, et al. Prediction of bone mineral density with dental radiographs. Bone 2007; 40: 1217-1221.

22. Verheij JGC, Geraets WGM, Van der Stelt PF, Horner K, Lindh C, Nicopoulou-Karayianni K, et al. Prediction of osteoporosis with dental radiographs and age. Dentomaxillofac Radiol 2009; 38: 431-437.

23. Geraets WGM, Verheij JGC, Van der Stelt PF, Horner K, Lindh C, Nicopoulou-Karayianni K, et al. Selecting regions of interest on intraoral radiographs for the prediction of bone mineral density. Dentomaxillofac Radiol 2008; 37: 375-379.

24. Geraets WGM, Van der Stelt PF, Elders PJM. The radiographic trabecular bone pattern during menopause. Bone 1993; 14: 859-864.

25. Geraets WGM, Van der Stelt PF, Lips P, Van Ginkel FC. The radiographic trabecular pattern of hips in patients with hip fractures and in elderly control subjects. Bone 1998; 22: 165-173.

26. Geraets WGM. Comparison of two methods for measuring orientation. Bone 1998; 23: 383-388.

27. Geraets WGM, Verheij JGC, Van der Stelt PF, Horner K, Lindh C, Karayianni K, et al. Osteoporosis and the general dental practitioner: reliability of some digital dental radiological measures. Community Dent Oral Epidemiol 2007; 35: 465-471.

28. Lee BD, White SC. Age and trabecular features of alveolar bone associated with osteoporosis. Oral Surg Oral Med Oral Pathol Oral Radiol Endod 2005; 100: 92-98.

29. White SC, Rudolph DJ. Alterations of the trabecular pattern of the jaws in patients with osteoporosis. Oral Surg Oral Med Oral Pathol Oral Radiol Endod 1999; 88: 628-635.

30. White SC, Cohen JM, Mourshed FA. Digital analysis of trabecular pattern in jaws of patients with sickle cell anemia. Dentomaxillofac Radiol 2000; 29: 119-124.

31. White SC. Oral radiographic predictors of osteoporosis. Dentomaxillofac Radiol 2002; 31: 84-92.

32. White SC, Atchison KA, Gornbein JA, Nattiv A, Paganini-Hill A, Service SK, et al. Change in mandibular trabecular pattern and hip fracture rate in elderly women. Dentomaxillofac Radiol 2005; 34: 168-174.

33. Cendre E, Kaftandjian V, Peix G, Jourlin M, Mitton D, Babot D. An investigation of segmentation methods and texture analysis applied to tomographic images of human vertebral cancellous bone. J Microsc 2000; 197: 305-316.

34. Chen H, Zhou X, Shoumura S, Emura S, Bunai Y. Age- and gender-dependent changes in three-dimensional microstructure of cortical and trabecular bone at the human femoral neck. Osteoporos Int 2010; 21: 627-636.

35. Homminga J, Mccreadie BR, Weinans H, Huiskes R. The dependence on the elastic properties of osteoporotic cancellous bone on volume fraction and fabric. J Biomech 2003; 36: 1461-1467.

36. Licks R, Licks V, Ourique F, Radke Bittencourt H, Fontanella V. Development of a prediction tool for low bone mass based on clinical data and periapical radiography. Dentomaxillofac Radiol 2010; 39: 224–230.

37. Rizzoli R. Microarchitecture in focus. Osteoporos Int 2010; 21: S403-S406.

38. Thomsen JS, Laib A, Koller B, Prohaska S, Mosekilde Li, Gowin W. Stereological measures of trabecular bone structure: comparison of 3D micro computed tomography with 2D histological sections in human proximal tibial bone biopsies. J Microsc 2005; 218: 171-179.

39. Zhang ZM, Li ZC, Jiang SD, Dai LY. Micro-CT and mechanical evaluation of subchondral trabecular bone structure between postmenopausal women with osteoarthritis and osteoporosis. Osteoporos Int 2010; 21: 1383-1390.

40. Hays WL. Statistics. 4th ed. Holt, Rinehart and Winston Inc. 1988. ISBN 0-03-022992-8

41. Nackaerts O, Jacobs R, Devlin H, Pavitt S, Bleyen E, Yan B, et al. Osteoporosis detection using intraoral densitometry. Dentomaxillofac Radiol 2008; 37: 282-287.

Figures

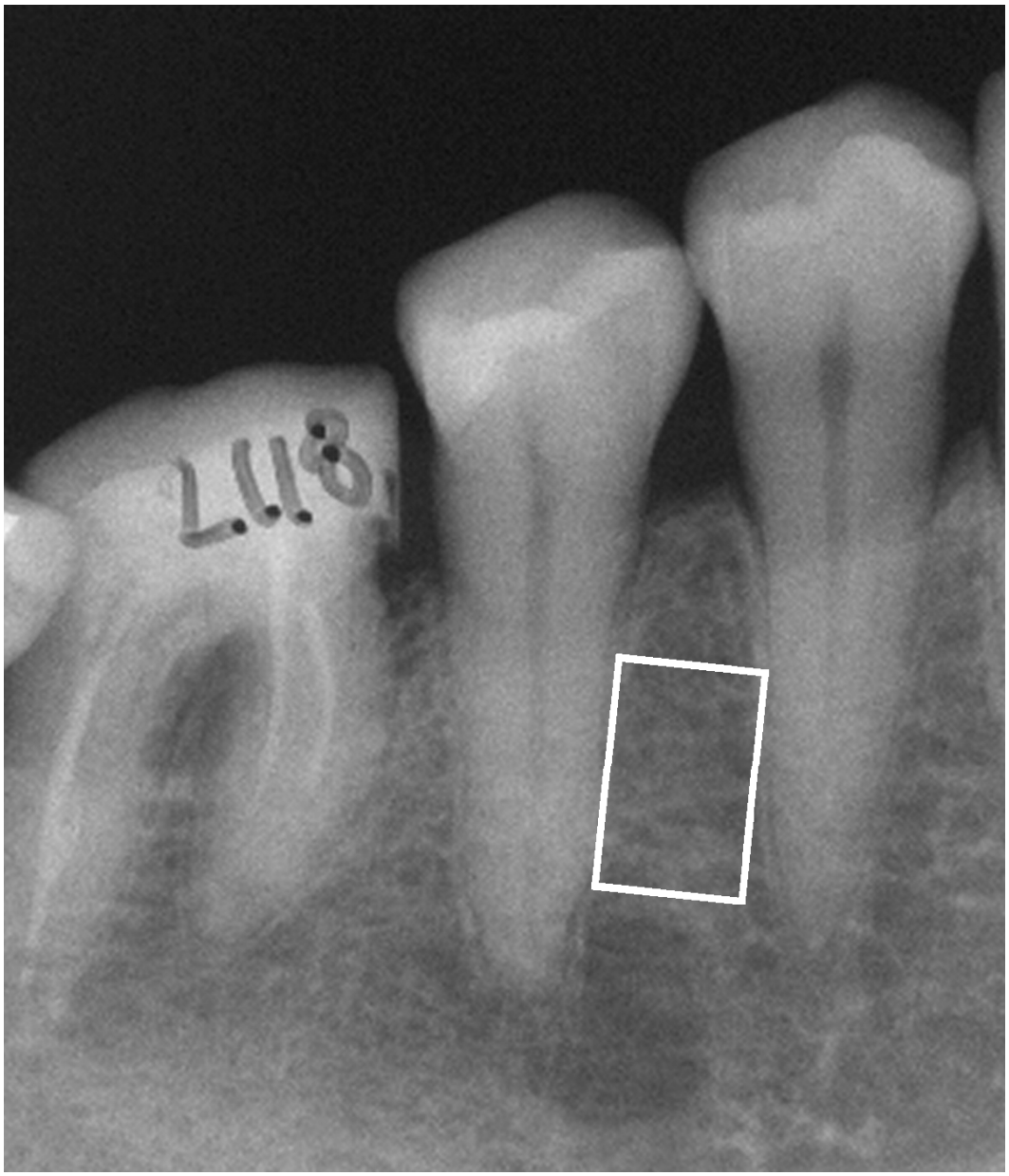

Figure 1: Radiograph of the right side of the lower jaw with region of interest 3.7 mm x 5.8 mm between first and second premolar. This is used to measure mean and standard deviation of the gray value (MEAN, SD).

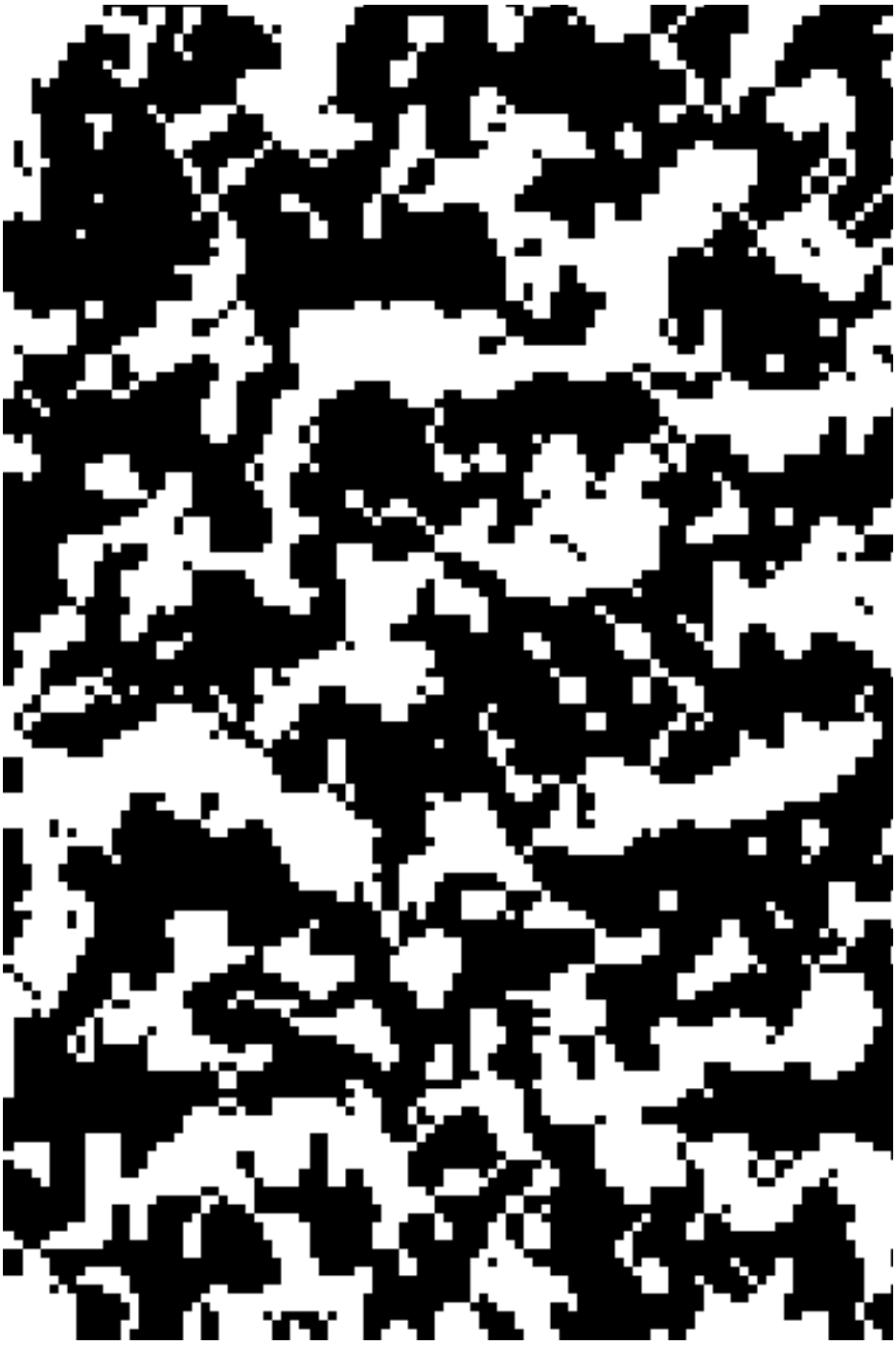

Figure 2: The region of interest in fig.1 has been filtered and segmented into black and white segments. This is used to measure fractal dimension (FRACT), numbers of black and white segments ($N_{black,}$ N_{white}), area and perimeter of the white segments (BV/TV, BS/TV) and orientation (LFD 0, LFD 15, ..., LFD 165).

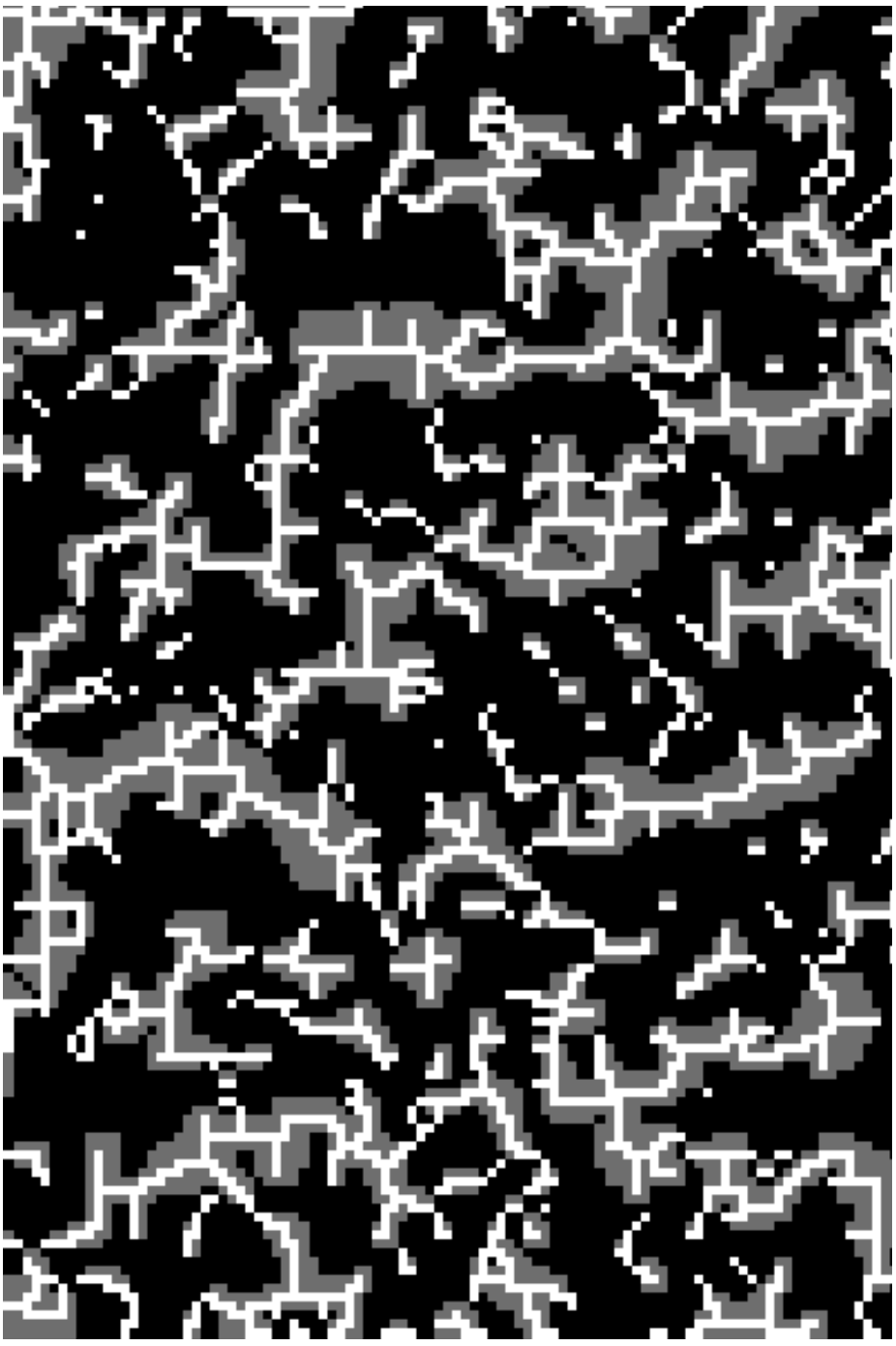

Figure 3: The white segments in fig.2 have been eroded. The eroded parts are displayed in gray. The remaining wire structure is displayed in white. Each white pixel contributes to the length of the white frame (TSL_{white}). Each white pixel with 1 (or 0) white neighbours is an endpoint and contributes to $N.Tn_{white}$. Each white pixel with 3 (or 4) white neighbours is a furcation point and contributes to $N.Nd_{white}$.

Table 1: Correlations between observer grading and image features.

Feature	Codename	Upper jaw	Lower jaw
average grayvalue	MEAN	-0.37	-0.39
standard dev of gray value	SD	-0.10	-0.13
fractal dimension	FRACT	+0.16	+0.09
number of white segments	N_{white}	+0.15	+0.11
number of black segments	N_{black}	-0.18	-0.18
area of white segments	BV/TV	-0.19	-0.26
perimeter white segments	BS/TV	-0.16	-0.32
orientation horizontal	LFD 0	ns	+0.12
orientation along 15°	LFD 15	ns	ns
orientation along 30°	LFD 30	ns	ns
orientation along 45°	LFD 45	ns	-0.13
orientation along 60°	LFD 60	-0.14	-0.18
orientation along 75°	LFD 75	-0.15	-0.19
orientation vertical	LFD 90	-0.13	-0.16
orientation along 105°	LFD105	-0.10	-0.15
orientation along 120°	LFD120	-0.11	ns
orientation along 135°	LFD135	ns	ns
orientation along 150°	LFD150	ns	+0.11
orientation along 165°	LFD165	ns	+0.11
length white wire	TSL_{white}	-0.21	-0.32
endpoints white wire	$N.Tn_{white}$	ns	ns
furcations white wire	$N.Nd_{white}$	-0.14	-0.19
length black wire	TSL_{black}	ns	ns
endpoints black wire	$N.Tn_{black}$	-0.19	-0.22
furcations black wire	$N.Nd_{black}$	-0.09	ns

ns = not significant.

Table 2: Results of stepwise multiple linear regression.

Upper jaw

Order in regression	Feature in upper jaw	Codename	Variance accounted for
1	average grayvalue	MEAN	14%
2	perimeter white segments	BS/TV	16%
3	orientation along 75°	LFD 75	18%
4	standard dev of gray value	SD	19%

Lower jaw

Order in regression	Feature in lower jaw	Codename	Variance accounted for
1	average grayvalue	MEAN	15%
2	perimeter white segments	BS/TV	21%
3	orientation along 75°	LFD 75	23%
4	length of white wire	TSL_{white}	25%
5	orientation horizontal	LFD 0	26%
6	furcations white wire	$N.Nd_{white}$	27%

Stepwise multiple linear regression first selects the single feature describing the observer grading best. The second feature is selected to increase descriptive power the most. This is continued as long as significant improvement can be achieved.